Supplement of Clim. Past, 12, 961–979, 2016
http://www.clim-past.net/12/961/2016/
doi:10.5194/cp-12-961-2016-supplement

Climate of the Past
Open Access
EGU

Supplement of

The influence of volcanic eruptions on the climate of tropical South America during the last millennium in an isotope-enabled general circulation model

Christopher M. Colose et al.

Correspondence to: Christopher M. Colose (ccolose@albany.edu)

Supplemental Figure Captions

Fig. S1. Number of rain gauges per grid box for selected months (during eruption events) in the GPCCv6 network. Bottom right panel shows a time-series of the total number of stations over the range 90° to 30° W and 60°S to 20° N.

Fig. S2. Zonally averaged latitudinal AOD distribution for all 15 events used in each ensemble member for DJF. Mean of all curves shown in red.

Fig. S3. As in Figure S2, but for JJA.

Fig. S4. Precipitation anomaly (mm day^{-1}) for each volcanic eruption used in LM composite (each averaged for the three ensemble members used) during DJF.

Fig. S5. As in Figure S4, but for JJA.

Fig. S6. Global-scale precipitation anomaly (mm day^{-1}) in the LM composite for (top) DJF and (bottom) JJA.

Fig. S7. Regression of spatially-averaged DJF $\delta\,^{18}O_p$ anomaly vs. temperature (black squares) or precipitation (red squares). The regression uses all 45 LM volcanic events and averaging is done over the SAMS domain defined in the text. Black and red lines are the corresponding (least-squares) regression lines.

Fig. S8. a) DJF total $\delta^{18}O_p$ anomaly **b)** DJF $\delta^{18}O_p$ anomaly due to isotopic composition change in precipitation, holding precipitation seasonality fixed at pre-eruption values. **c)** As in a) except for JJA. **d)** As in b) except for JJA. Total isotopic changes in left column reproduced from Figure 10 in text.

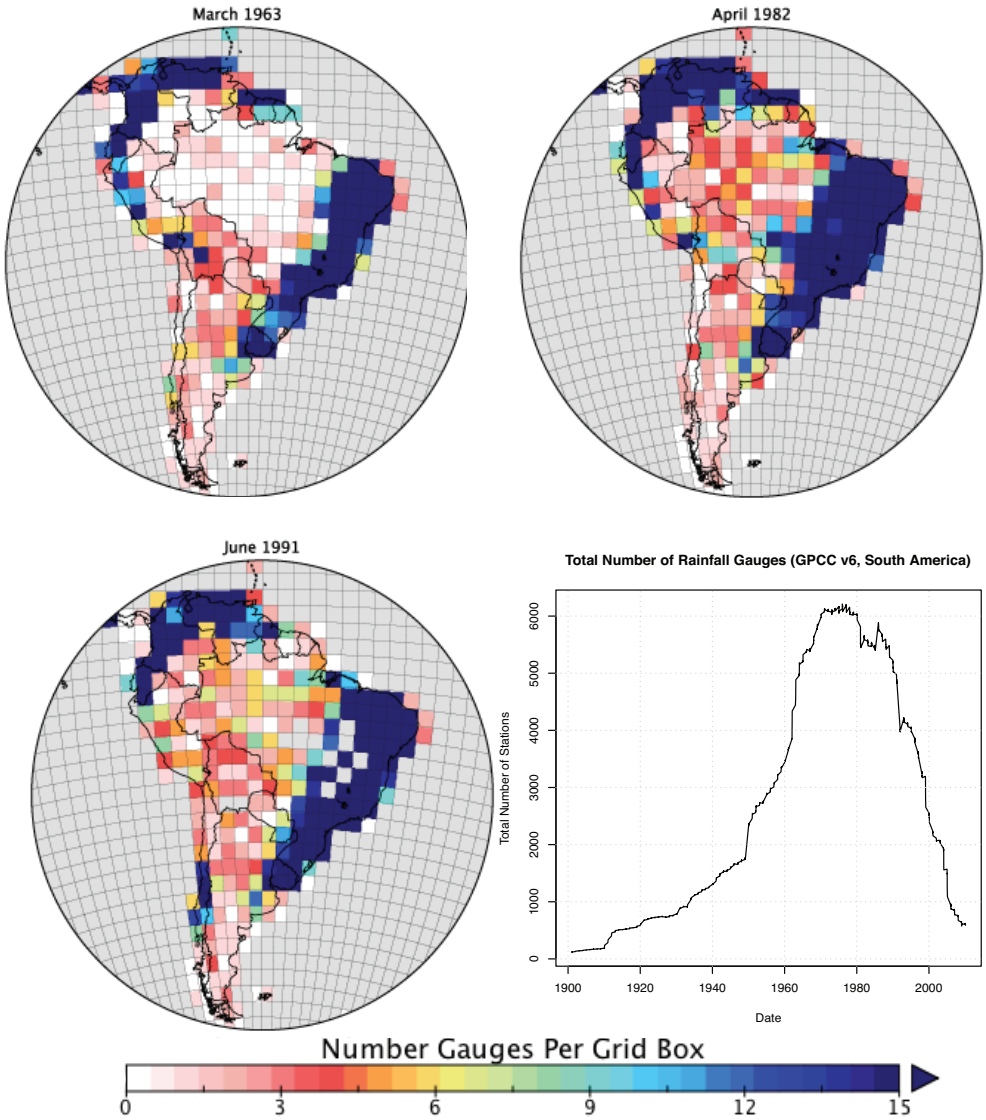

Fig. S1. Number of rain gauges per grid box for selected months (during eruption events) in the GPCCv6 network. Bottom right panel shows a time-series of the total number of stations over the range 90° to 30° W and 60°S to 20° N.

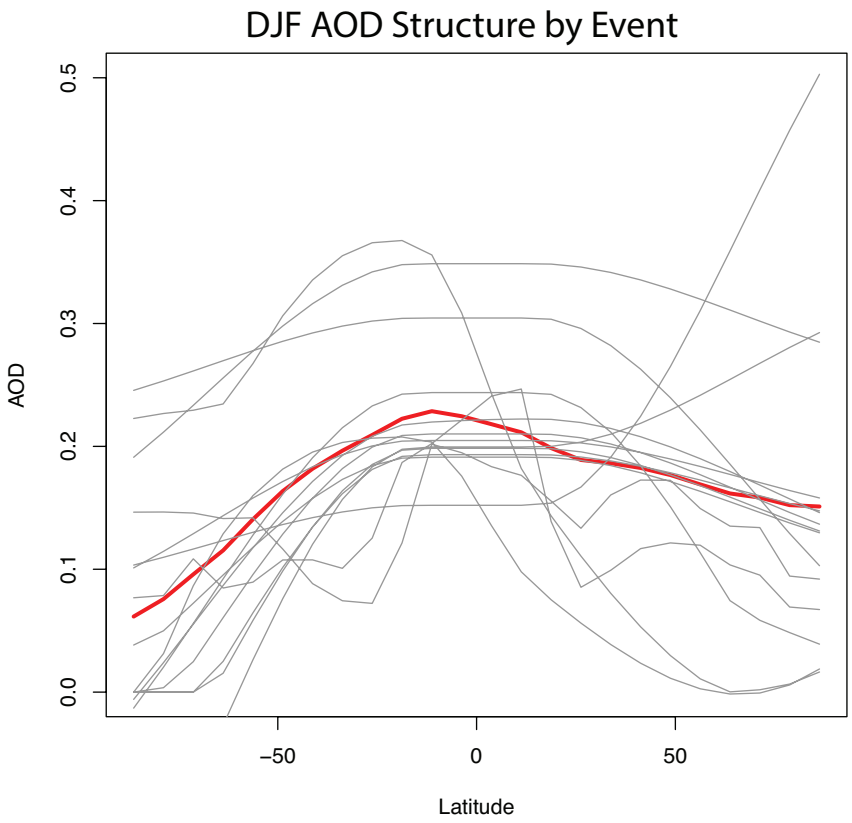

Fig. S2. Zonally averaged latitudinal AOD distribution for all 15 events used in each ensemble member for DJF. Mean of all curves shown in red.

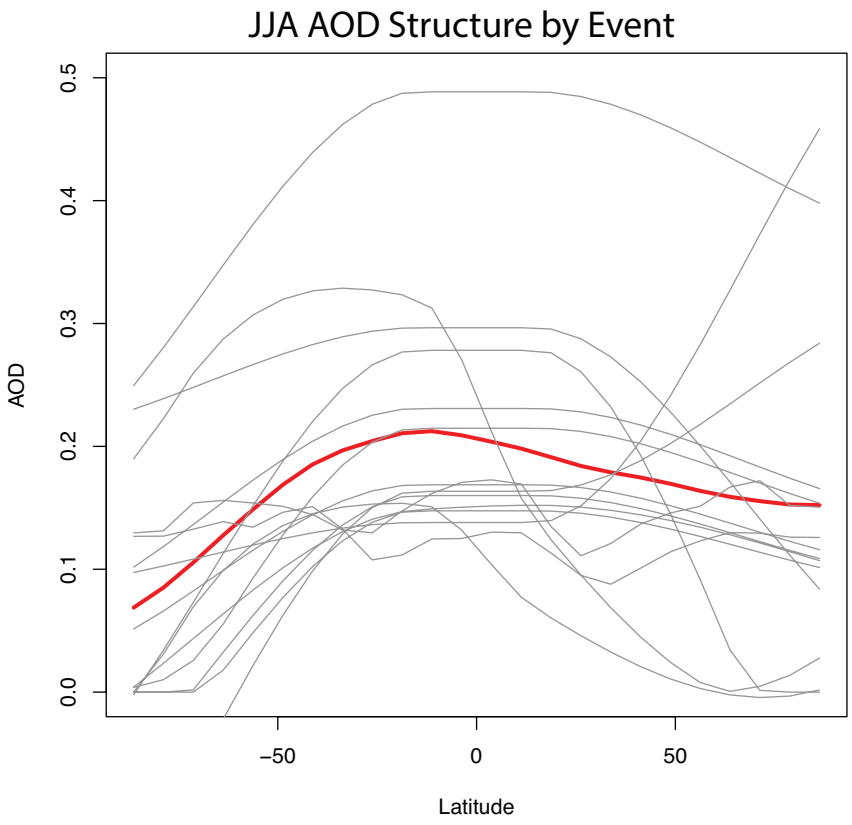

Fig. S3. As in Figure S2, but for JJA.

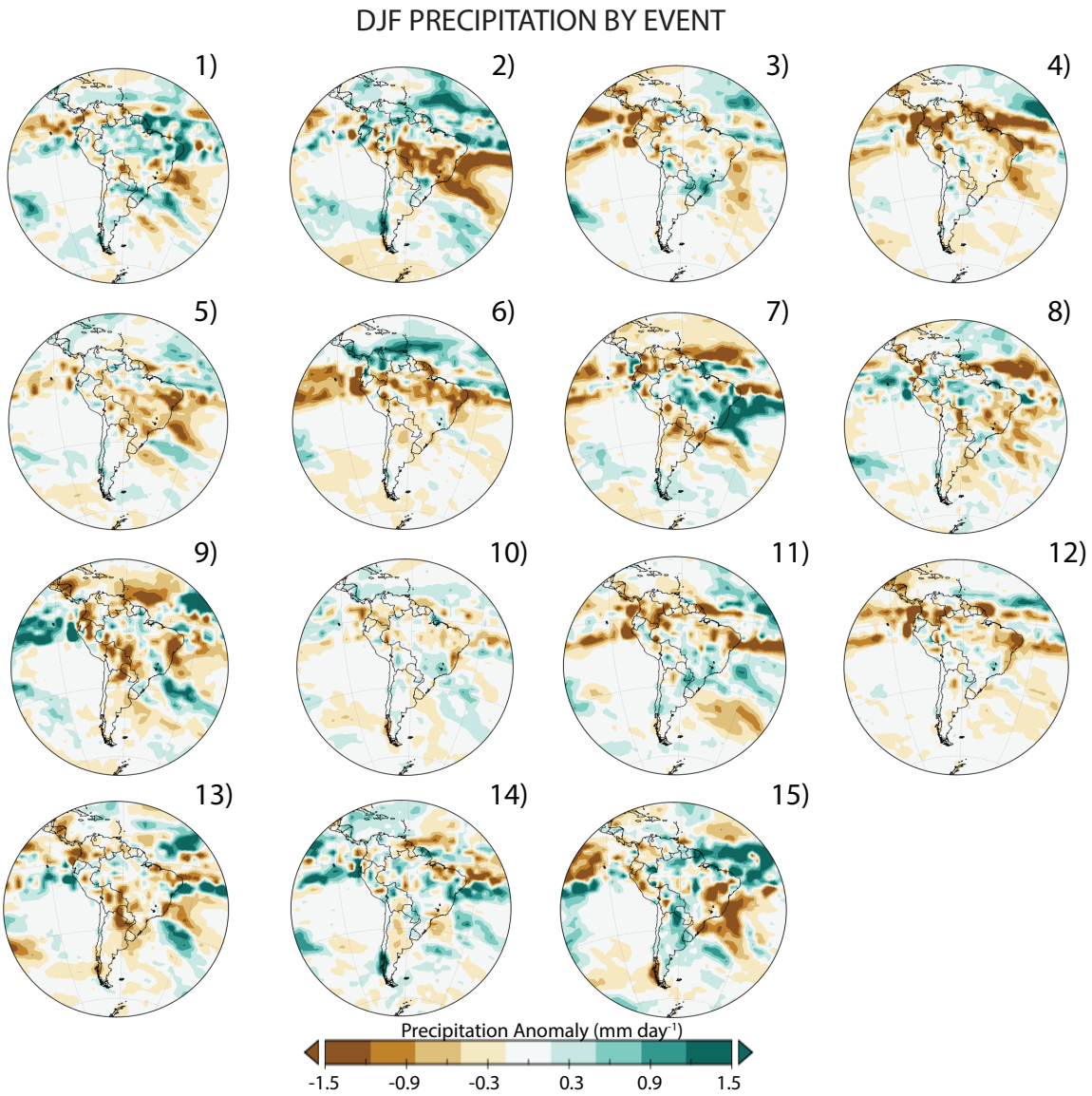

Fig. S4. Precipitation anomaly (mm day^{-1}) for each volcanic eruption used in LM composite (each averaged for the three ensemble members used) during DJF.

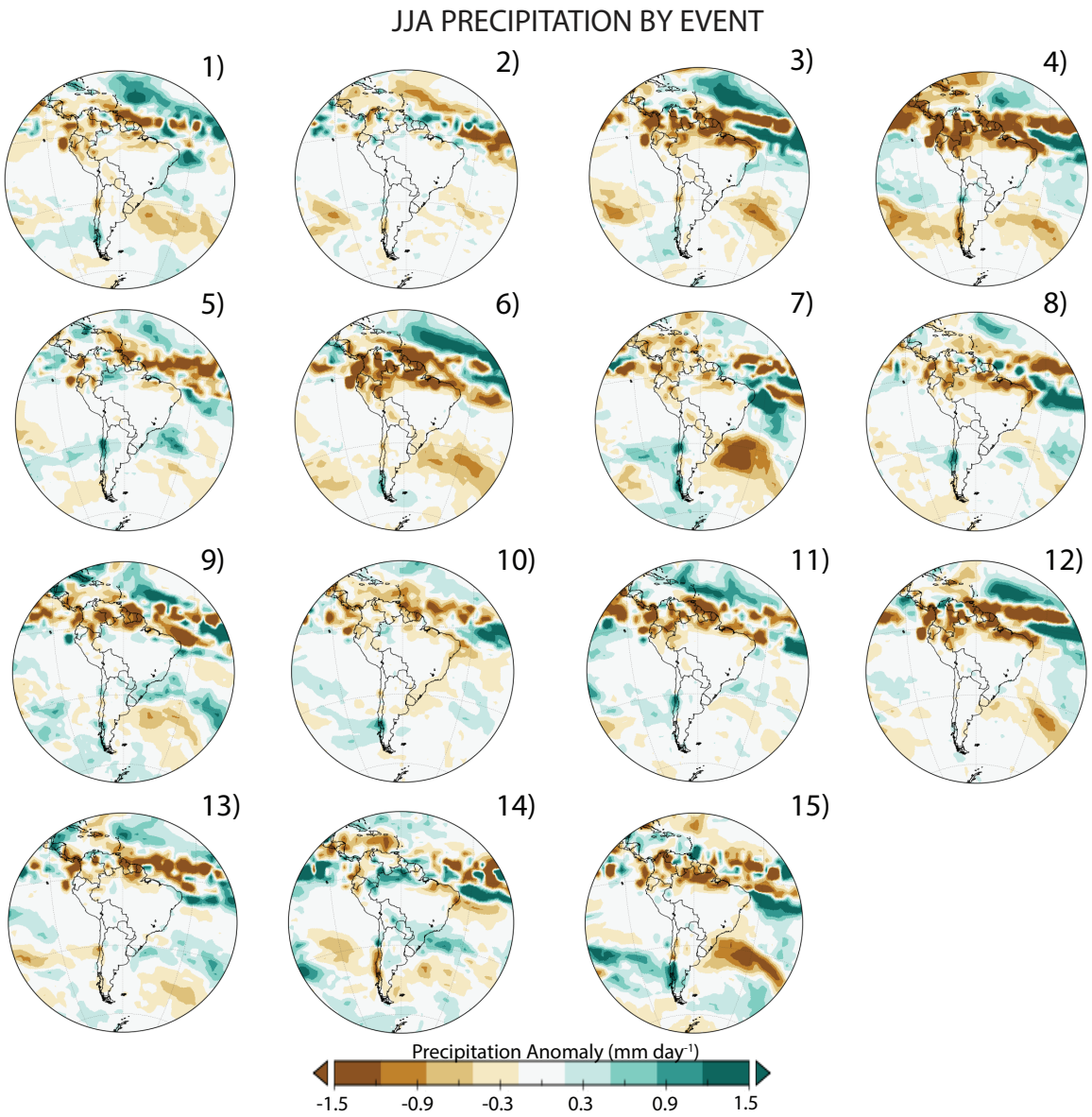

Fig. S5. As in Figure S4, but for JJA.

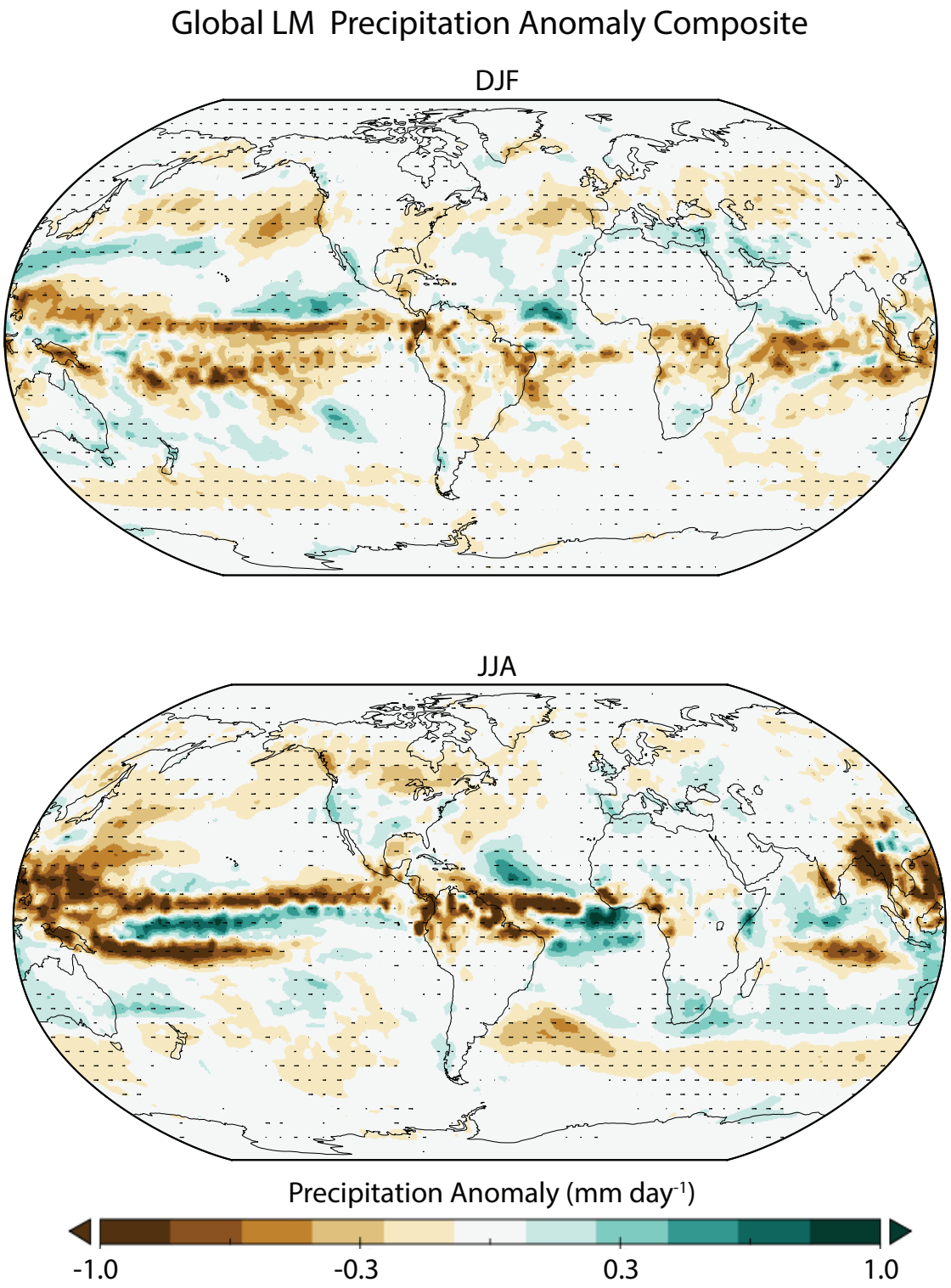

Fig. S6. Global-scale precipitation anomaly (mm day^{-1}) in the LM composite for (top) DJF and (bottom) JJA.

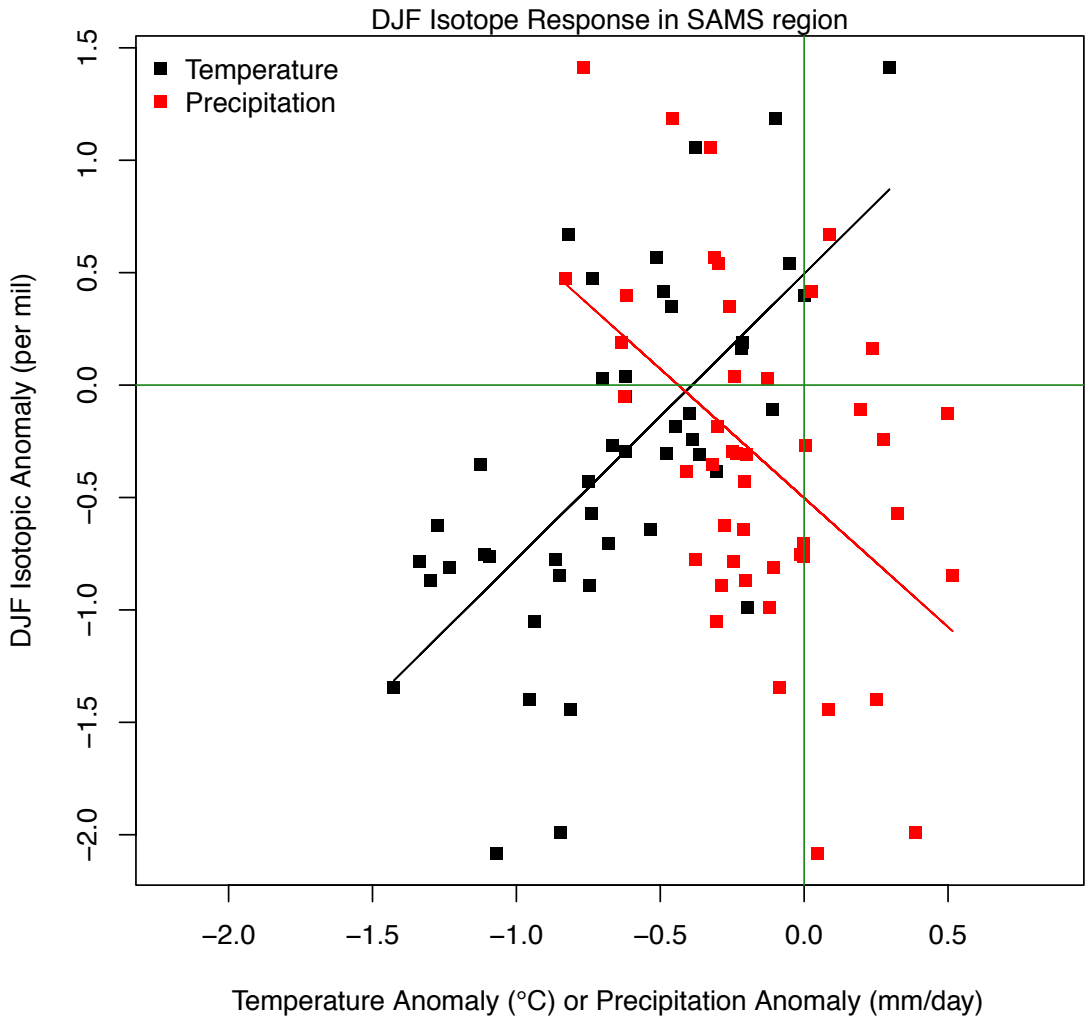

Fig. S7. Regression of spatially-averaged DJF $\delta\,^{18}O_p$ anomaly vs. temperature (black squares) or precipitation (red squares). The regression uses all 45 LM volcanic events and averaging is done over the SAMS domain defined in the text. Black and red lines are the corresponding (least-squares) regression lines.

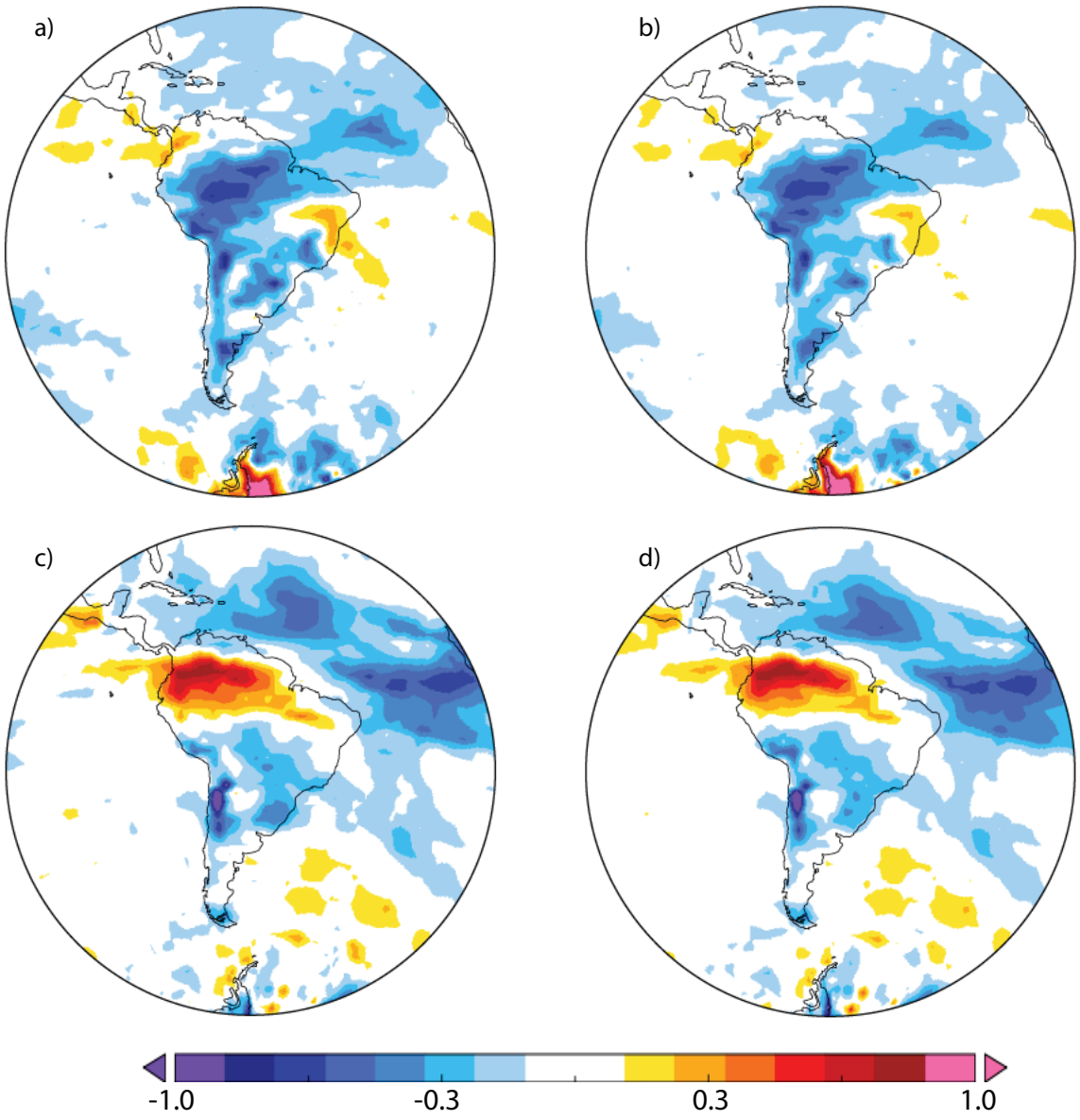

Fig. S8. a) DJF total $\delta^{18}O_p$ anomaly **b)** DJF $\delta^{18}O_p$ anomaly due to isotopic composition change in precipitation, holding precipitation seasonality fixed at pre-eruption values. **c)** As in a) except for JJA. **d)** As in b) except for JJA. Total isotopic changes in left column reproduced from Figure 10 in text.